Bull. Nov. Comp. Center, Math. Model. in Geoph., 5 (1999), 1–19

Simultaneous identification of two coefficients in a diffusion equation*

A.V. Avdeev, E.V. Goryunov, M.M. Lavrentiev, Jr., R. Spigler

An algorithm for the simultaneous determination of *two* coefficients in an inverse problem for equations of the parabolic type is presented. The model under investigation has been proposed in the literature to describe the long-time coastal profile evolution. The iterative inversion procedure is based on the minimization of a suitable cost functional. Such a functional is considered in terms of the Laplace transforms of the solution to the original dynamical problem. Results of numerical tests are also shown to illustrate the performance of the algorithm.

1. Introduction

This paper is devoted to the numerical treatment of a two-coefficient inverse problem for a certain linear parabolic differential equation. Inverse problems for hyperbolic governing equations have been rather well studied in view of various applications, such as, e.g., Seismology and Electrodynamics. Without going into details, we refer the reader to the specialized literature, see for instance [1–3]. However, a comparatively small number of publications still deal with parabolic problems, even though such problems arise in a number of applications too. For example, the long-term coastal profile evolution could be described in terms of diffusion–transport type model [4, 5].

In order to better describe the content of the paper, we formulate first one of the simplest inverse problem which corresponds to a version of the 1D Lamé system (see [6], e.g.). Consider the following problem:

$$u_{tt} = \left(D(z)u_z\right)_z \qquad \text{for} \quad t > 0, \quad z \geq 0, \tag{1.1}$$

$$u|_{t<0} \equiv 0, \qquad u_z|_{z=0} = \delta(t), \tag{1.2}$$

where $\delta(t)$ represents the Dirac delta function, while the coefficient $D(z)$ corresponds to the elastic properties of the medium (for example, the velocity of longitudinal or shear waves). In case when additional (measured) data at the free surface are available,

*Partially supported by the Russian Foundation for Basic Research, under Grants 99-05-64538, 99-05-65372, 98-05-65280, UNESCO under contract UVO-ROSTE 875.629.9, and the PACE-MAST III EU project.

$$u|_{z=0} = u_0(t), \tag{1.3}$$

an inverse problem could be formulated as follows:

Inverse Problem 1 (IP1). *Given the function $u_0(t)$, find the unknown function $D(z)$ (in a certain functional space), such that the solution $u(z,t)$ to* (1.1), (1.2) *satisfies the additional condition* (1.3).

An approach widely used for the numerical study of this problem, is based on iterative procedures for the minimization of some cost functional, with the help of optimization methods, such as steepest descent, conjugate gradient methods, quasi-Newton methods, e.g. In case of IP1, the cost functional could be constructed in the following way. Choose, as a first guess, an approximated diffusion coefficient, solve the direct problem (1.1), (1.2), find the trace of solution, $u(z,t)$ at the point $z = 0$, and introduce the cost functional

$$\Phi[D(z)] = \int_0^\infty |u_0(t) - u(0,t)|^2 \, dt + \beta \sup_z \left| D(z) - D^{\text{est}} \right|, \tag{1.4}$$

β being the regularization parameter, and $D^{\text{est}}(z)$ (the "estimated" $D(z)$) is defined by the physical properties of the medium under study. We assume that the global minimum of this functional corresponds to the solution of IP1.

In view of Parseval identity, the functional $\Phi[D]$ in (1.4) can be minimized in the so-called "frequency domain". The frequency variable, which has a clear physical meaning, for example in geophysical problems [1], is nothing but the dual variable after the Fourier transforming the problem with respect to time, t.

Let now consider a similar inverse problem but for the parabolic governing equation:

Inverse Problem 2 (IP2). *Given the function $v_0(t)$, find* **two** *functions, $D(z)$ and $B(z)$, such that the solution $v(z,t)$ to the problem*

$$\begin{aligned} &v_t = D^2(z) v_{zz} + B(z) v \quad \text{for} \quad t > 0, \quad 0 \le z \le H, \\ &v|_{t=0} = 0, \quad v_z|_{z=0} = \phi_1(t), \quad v|_{z=H} = 0 \end{aligned} \tag{1.5}$$

satisfies the additional condition $v|_{z=0} = v_0(t)$.

Clearly, the present problem differs from the IP1 for several reasons. First of all, (i) the model equation is of the diffusion type; (ii) there are two unknown coefficients to be recovered; (iii) the space interval is bounded. Nevertheless, we shall use a similar approach, namely minimization of some cost functional, in the frequency domain, to solve the IP2. Therefore, in addition to points (i)–(iii) above, we have some other peculiarities. Taking the Laplace transform of equation (1.5), we obtain an Helmholtz equation, similar to that obtained in the IP1 after a Fourier transform. However, in this case we do not have the tool of the Parseval equality, and existence of the Laplace transform of solutions is part of the problem. Note that we do not need to resort to the inverse Laplace transform at the end, since the coefficients D and B only depend on the space variable, and thus the reconstruction of D and B can be obtained remaining in the frequency domain.

In this paper, we provide some partial answers to the questions above, and demonstrate some numerical results of the inversion procedure. We also expect to be able to process numerically some of the measured (real) data in the nearest future. The rest of the paper is organized as follows. In Section 2, we give an extended introduction to the diffusion-type models which describe long-term coastal profile evolution. Our understanding is that most of mathematicians interested in Inverse Problems are not yet acquainted with such an important area of applications. As is proved in Section 3, at least in the case of constant coefficients, D and B in (1.5), the Laplace transform of the solution to equation (1.5) does exist. In Section 4, we describe some modification of the conjugate gradient method, to minimize the relevant cost functional, and give some results of the numerical tests.

2. Diffusion models for the long-term coastal profile evolution

Erosion and accretion phenomena are responsible for modifications to the coastal environment, and thus have been a source of growing concern among coastal engineers. These modifications occur, in some cases, as artificial structures, such as, e.g., groins or seawalls, are built, to protect against severe wave action for harbors, or to alleviate the effects of erosion on adjacent shore property. They may arise as a result of human activities needed to exploit natural resources (e.g., artificial sand islands created to be used as drilling platforms for oil exploration). In any case the newly introduced structure disturbs the dynamic equilibrium of sediment transport and thus alters the coastal morphology. In order to minimize possible undesirable effects due to this alteration, it is necessary to investigate the consequent changes in coastal morphology.

There are in general two basic approaches adopted in coastal engineering to study this problem, namely:

1. Hydraulic (physical) models;
2. Mathematical models.

In the case of *hydraulic model* studies, a small-scale laboratory model (a prototype) is constructed for the problem under study. From this study, projections are made about the expected behavior of the prototype. Even though several problems may arise in such investigations due to scale effects, the results obtained are valuable in understanding the various mechanisms acting on the coastal environment. However, such physical models are usually very expensive and require observations extended over a long time if a number of options are to be tested.

Since, however, high speed computers are becoming available as well as a deeper understanding of the coastal processes, the *mathematical simulation* is becoming a major tool in coastal engineering as in many other fields.

It should be stressed that the various processes involved can occur over different time- and space-scales, namely:

1. Small-scale coastal behavior;
2. Meso-scale coastal behavior (over a period of months to a few decades);
3. Large-scale coastal behavior (over a period of decades to a few centuries);
4. Meta-scale coastal behavior (geological evolution of the coastal plain over centuries to millennia).

These time scales can be divided into *long-term* and *short-term* processes. Short-term processes are rather well studied by hydraulic (hydrodynamic) models, while long-term modeling of coastal behavior is still far from being satisfactory.

Even if we would have a sufficient computing power to run small-scale models for a sufficiently long period of time, this might be not the best approach for long-term modeling. Processes which are negligible at smaller scale may have significant long-term effects and conversely. Therefore, it is important to study long-term processes regardless of the short-term processes.

As a result of the complexity of the coastal processes, the coastal engineers usually proceed by simplifying the processes themselves into a number of modules which can be formulated separately. The results are then assembled together in a quasi-steady process, to form the required model. For example, the coastal phenomena involved in morphology development, have been simplified into a 3-stage process of wave transformation, sediment transport, and erosion/accretion (morphology development), see [5].

The largest and most consistent body of work concerns coastline models [7], and the equilibrium state of the system, for example, the equilibrium coastal profiles [8].

One of the key elements in the long-term modeling, is reduction of information. For example, we need to operate a data reduction which enables us to separate the relevant information from the "noise", and to reduce this to a tractable (low) number of parameters. For quite a long time, these two sources of information have been separated, namely, investigations were made either from an empirical point of view, or from a process-based modeling.

The reduction of information involves essentially four levels, which concern input, physical system (or its model), output, and interpretation (or generalization). These levels are reflected in the various approaches to long-term modeling:

1. Input reduction, based on the idea that we can describe long-term residual effects (e.g. transport fields) with models based on the description of small-scale processes.
2. Model reduction, based on the idea that, by using more or less formal analysis and integration methods, the model might be reformulated at the scale of interest, without describing all details of smaller-scale effects.
3. Behavior-oriented modeling which attempts to describe the phenomena without going into the underlying process.

All of these approaches have been discussed, for instance, in [5].

The problem of quantization is important in coastal profile modeling. Usually, the area under investigation is discretized by a rectangular grid, using fixed along-shore and cross-shore meshes. Here the depth is allowed to vary in each grid according to a condition of continuity for sediment transport. To ensure that the depths are continuous along grid lines, changes in depth along these lines are found by averaging between adjacent grids. In an alternative method, the area of studies is divided into a fixed number of cross-shore strips. Each strip can be analyzed as a single computational cell, or can be further divided into multiple cells. For computation related to morphology, the section of the profile within each cell is assumed to accrete or be eroded uniformly (i.e., the profile translates), in such a way that the total accretion/erosion equals the net sediment transport into the cell. The movement of the contours between adjacent cells are found by linear interpolation.

In the quantitization above, if each strip is analyzed as one single cell, the whole profile is assumed to move uniformly, and the model is called a *1-line model* [9]. In this case, the cross-shore length of the strip should be extended only to the critical depth (depth at which sediment transport is negligible). In the sequel, such a depth will be referred to as *the depth of closure.*

Alternatively, if each strip is divided into N cells, the profile is divided into N segments, and each profile segment is used to translate the net sediment transport into each cell as accretion/erosion. In this case, the model becomes a *N-line model* [10]. In order to evaluate the morphology changes in each cell, it is necessary to compute the sediment transport at the ends of each cell.

In the paper [9], diffusion equations have been derived applying mass conservation to the 1-line model of coastal profile. The diffusion coefficient in the governing equation, having the physical dimension of a square length divided by time, corresponds to the time scale of shoreline change, following a disturbance (a wave action). A high amplitude of the long-shore sand transport rate produces a rapid shoreline response, so that a new state of equilibrium with the incident waves is attained. Furthermore, a larger depth of closure indicates that a larger part of the beach profile participates in the sand movement, leading to a slower shoreline response.

Based on the aforementioned ideas, the following equation to describe long-term coastal profile evolution:

$$\frac{\partial(\delta X)}{\partial t} = D^2(z)\frac{\partial^2(\delta X)}{\partial z^2} + f\left(t, z, \delta X, \frac{\partial(\delta X)}{\partial z}\right). \tag{2.1}$$

This equation has been introduced in [5]. Here, $\delta X(z,t)$ represents the change of cross-shore position of the coastal profile, $D(z)$ is the diffusion coefficient, and z is the distance from the shoreline.

Let give some explanations for the special case of the term $f(t, z, \delta X, \frac{\partial(\delta X)}{\partial z})$. If $f = S(z,t)$, it is possible to introduce the effects of a random forcing, long-shore transport gradients, and human inference, such as nourishment and sand mining [5]. The choice $f = B(z)\frac{\partial(\delta X)}{\partial z}$, or $f = B(z)\delta X$, is also interesting in view of applications. In these models, the coefficient $B(z)$ represents the velocity of long-shore sand waves movement. Thus, the collective movement of long-shore sand waves can be described in addition to a particular movement. This means that the sediment motion is characterized by two scales: a relatively rapid movement of sand particles, and a relatively slow collective movement of sand bodies. Clearly, all process-based and empirical knowledge is stored in the coefficients $D(z)$ and $B(z)$ as well as in the boundary conditions.

In this paper, we assume that $f = B(z)\delta X$ in (2.1). Therefore, consider the

Inverse Problem 3. *Suppose the function $\delta X(z,t)$ (the cross-shore position of the coastal profile) solves*

$$\frac{\partial(\delta X)}{\partial t} = D^2(z)\,\frac{\partial^2(\delta X)}{\partial z^2} + B(z)\,\delta X, \tag{2.2}$$

$$\delta X|_{t=0} = 0, \tag{2.3}$$

$$\left.\frac{\partial(\delta X)}{\partial z}\right|_{z=0} = \varphi_0, \qquad \delta X|_{z=H} = 0. \tag{2.4}$$

We want to reconstruct the unknown coefficients, $D(z)$ and $B(z)$, using the additional information (measurements at the observation surface $z = 0$)

$$\delta X\big|_{z=0} = \delta X_0. \tag{2.5}$$

3. Theoretical background

To study the inverse problem above we use the formal Laplace transform. Reformulating original problem in such a way we obtain the inverse problem for the Helmholtz equation with parameter. It is necessary to develop some of the theoretical background.

For $(z,t) \in Q = [0,H] \times [0,\infty)$ consider the problem

$$u_t = D^2 u_{zz} + Bu, \tag{3.1}$$

$$u|_{t=0} = 0, \tag{3.2}$$

$$u_z|_{z=0} = \varphi_1(t), \qquad u|_{z=H} = 0, \tag{3.3}$$

$$u|_{z=0} = \varphi_0(t). \tag{3.4}$$

Problem (3.1)–(3.4) is similar to IP2. For convenience we use the notation $u = \delta X$. To give the desirable theoretical background we also suppose that $D = \text{const}$ and $B = \text{const}$.

Such direct problem is overdetermined. We consider this problem as an inverse problem, that is to find constants D and B having known $\varphi_0(t)$ and $\varphi_1(t)$.

In the sequel, we use the formal Laplace transform

$$v(z,\omega) = \int_0^\infty e^{\omega t} u(z,t)\, dt. \tag{3.5}$$

Here we show that in particular case under study such transform is correct. Let us study the spectrum of equation (3.1) with the homogeneous boundary conditions

$$u(0,t) = u(H,t) = 0. \tag{3.6}$$

Using the standard separation of the variables $u(z,t) = Z(z)T(t)$, we obtain the following boundary-value problem for the multiplier $Z(z)$:

$$Z'' + \frac{B-\lambda}{D^2} Z = 0, \qquad Z(0) = Z(H) = 0,$$

that, obviously, possesses nontrivial solution for

$$\frac{B-\lambda}{D^2} = \frac{n^2\pi^2}{H^2},$$

or, what is the same, for

$$\lambda_n = B - \frac{n^2\pi^2}{H^2}D^2.$$

Thus, the very right eigenvalue of problem (3.1), (3.6) is as follows:

$$\lambda_1 = B - \frac{\pi^2}{H^2}D^2. \tag{3.7}$$

As well-known, for any initial function $u(z,0) = u_0(z) \in L_2(0,H)$ satisfying the compatibility conditions, $u_0(0) = u_0(H) = 0$, solution to problem (3.1), (3.6) satisfies the estimate

$$\sup_{z\in[0,H]} |u(z,t)| \le K\, e^{\lambda_1 t}.$$

Therefore, the Laplace transform (3.5) is valid for

$$\omega < -\lambda_1. \tag{3.8}$$

Due to homogeneous initial condition (3.4) for the values of ω satisfying (3.8), we have

$$\int_0^\infty e^{\omega t} u_t(z,t)\, dt = e^{\omega t} u\Big|_{t=0}^{\infty} - \omega \int_0^\infty e^{\omega t} u\, dt = -\omega v(z,\omega).$$

Thus, assuming the proper behavior of the functions $\varphi_i(t)$ as $t \to \infty$, after using the Laplace transform with ω satisfying (3.8) from (3.1)–(3.4), we obtain the following problem for the Helmgoltz equation with a parameter

$$\frac{d^2 v(z,\omega)}{dz^2} + \frac{B+\omega}{D^2} v(z,\omega) = 0, \tag{3.9}$$

$$\frac{dv}{dz}\Big|_{z=0} = h_1(\omega), \qquad v|_{z=H} = 0, \tag{3.10}$$

$$v_{z=0} = h_0(\omega), \tag{3.11}$$

where $h_i(\omega) = \int_0^\infty e^{\omega t}\varphi_i(t)\, dt$.

For $\omega > -B$, i.e., for (cf. (3.7) and (3.8))

$$\omega \in \left(-B, -B + \frac{\pi^2}{H^2}D^2\right), \tag{3.12}$$

the general solution to the ODE (3.9) with constant coefficients has the from

$$v(z,\omega) = C_1(\omega)e^{i\lambda z} + C_2(\omega)e^{-i\lambda z} \tag{3.13}$$

with

$$\lambda = \sqrt{\frac{B+\omega}{D^2}}. \tag{3.14}$$

Obviously,

$$\frac{dv(z,\omega)}{dz} = i\lambda\left[C_1(\omega)e^{i\lambda z} - C_2(\omega)e^{-i\lambda z}\right]. \tag{3.15}$$

Boundary condition (3.11) implies that

$$C_1(\omega)e^{iH\lambda} + C_2 e^{-iH\lambda} = 0,$$

or, what is the same, that

$$C_2(\omega) = -e^{2iH\lambda}C_1(\omega). \tag{3.16}$$

Thus, representation (3.13) takes the form

$$v(z,\omega) = C_1(\omega)\left[e^{i\lambda z} - e^{i\lambda(2H-z)}\right]. \tag{3.17}$$

Putting $z = 0$ in (3.17), we determine the multiplier $C_1(\omega)$ with the help of one of the functions $h_i(\omega)$ (see (3.10)). The other function h_j – "over-information" in view of general theory of the PDE – could be used for determination of the parameters D and B.

Indeed, from (3.10) and (3.17), we obtain that

$$h_0(\omega) = C_1(\omega)\left[1 - e^{2iH\lambda}\right], \tag{3.18}$$

and, moreover, that

$$h_1(\omega) = i\lambda\, C_1(\omega)\left[e^{i\lambda z} + e^{i\lambda(2H-z)}\right]\Big|_{z=0} = i\lambda\, h_0(\omega)\frac{1+e^{2iH\lambda}}{1-e^{2iH\lambda}}. \tag{3.19}$$

Summing up, let us write the ratio

$$\frac{h_1(\omega)}{h_0(\omega)} = i\lambda\frac{1+e^{2iH\lambda}}{1-e^{2iH\lambda}}. \tag{3.20}$$

Similar reasons could be used to treat the case of more general boundary conditions for equation (3.9). Here we are going to give all the necessary computations with a very few comments. For equation (3.9), consider the following problem

$$v|_{z=0} = h_0(\omega), \qquad v_z|_{z=0} = h_1(\omega), \tag{3.21}$$

$$v|_{z=H} = g_0(\omega), \qquad v_z|_{z=H} = g_1(\omega). \tag{3.22}$$

Using conditions (3.21) from representation (3.13), we get

$$\begin{aligned} C_1(\omega) + C_2(\omega) &= h_0(\omega), \\ i\lambda\,(C_1(\omega) - C_2(\omega)) &= h_1(\omega). \end{aligned}$$

Solving the above system, we obtain

$$C_1(\omega) = \frac{1}{2}\Big[h_0(\omega) + \frac{1}{i\lambda}h_1(\omega)\Big]; \quad C_2(\omega) = \frac{1}{2}\Big[h_0(\omega) - \frac{1}{i\lambda}h_1(\omega)\Big]. \tag{3.23}$$

Substituting formulae (3.23) into representation (3.13) we obtain the following system:

$$\begin{aligned} g_0(\omega) &= h_0(\omega)\frac{e^{iH\lambda} + e^{-iH\lambda}}{2} + \frac{h_1(\omega)}{i\lambda}\frac{e^{iH\lambda} - e^{-iH\lambda}}{2}, \\ g_1(\omega) &= i\lambda h_0(\omega)\frac{e^{iH\lambda} - e^{-iH\lambda}}{2} + h_1(\omega)\frac{e^{iH\lambda} + e^{-iH\lambda}}{2}. \end{aligned}$$

The later system could be rewritten as follows:

$$e^{iH\lambda} + e^{-iH\lambda} = 2\Big[i\lambda h_0^2 - \frac{h_1^2}{i\lambda}\Big]^{-1}\Big[i\lambda g_0 h_0 - \frac{g_1 h_1}{i\lambda}\Big], \tag{3.24}$$

$$e^{iH\lambda} - e^{-iH\lambda} = -2\Big[i\lambda h_0^2 - \frac{h_1^2}{i\lambda}\Big]^{-1}[g_0 h_1 - g_1 h_0]. \tag{3.25}$$

From (3.24) and (3.26) it is easy to obtain the relations

$$\begin{aligned} \frac{e^{iH\lambda} + e^{-iH\lambda}}{e^{iH\lambda} - e^{-iH\lambda}} &= \frac{1}{i\lambda}\frac{\lambda^2 g_0 h_0 + g_1 h_1}{g_0 h_1 - g_1 h_0}, \\ \frac{e^{iH\lambda} - e^{-iH\lambda}}{e^{iH\lambda} + e^{-iH\lambda}} &= i\lambda\frac{g_0 h_1 - g_1 h_0}{\lambda^2 g_0 h_0 + g_1 h_1}, \end{aligned} \tag{3.26}$$

similar to (3.20).

To calculate the integrals in (3.26), we use the residues theory. In (3.20), do the change (see (3.14))

$$z = e^{2iH\lambda} \quad \text{with} \quad \lambda = D^{-1}\sqrt{B+\omega}, \tag{3.27}$$

then, obviously

$$d\omega = 2D^2\lambda\, d\lambda, \qquad d\lambda = \frac{1}{2iH}\frac{dz}{z}. \tag{3.28}$$

Note that variation of ω within admissible interval (3.12) is corresponding to motion of new variable z in (3.27) along the unit circle of the complex plane $|z| = 1$ with $z = x + iy$. After the above change of variables (3.27), (3.28) from (3.26) we deduce that

$$\int_{\omega_0}^{\omega_1} \frac{h_0(\omega)}{h_1(\omega)}\,d\omega = \int_{\lambda(\omega_0)}^{\lambda(\omega_1)} \frac{1}{i\lambda}\frac{1-e^{2iH\lambda}}{1+e^{2iH\lambda}} 2D^2\lambda\,d\lambda$$

$$= -2iD^2 \int_{|z|=1} \frac{1-z}{1+z}\frac{1}{2iH}\frac{dz}{z} = -\frac{D^2}{H}\int_{|z|=1}\frac{1-z}{1+z}\frac{dz}{z}. \quad (3.29)$$

Similarly,

$$\int_{\omega_0}^{\omega_1} \frac{h_1(\omega)}{h_0(\omega)}\frac{d\omega}{B+\omega} = \frac{1}{H}\int_{|z|=1}\frac{1+z}{1-z}\frac{dz}{z}. \quad (3.30)$$

In order to calculate integrals (3.29) and (3.30), we claim that the unit circle $|z| = 1$ of the complex plane is passed exactly once clock otherwise. It means the following intervals of variation of the parameters ω and λ:

$$\lambda \in \left[\lambda_0,\, \lambda_0 + \frac{\pi}{H}\right), \qquad \omega \in \left[\omega_0,\, \omega_0 + \frac{\pi^2 D^2}{H^2}\right), \quad (3.31)$$

which corresponds to assumption (3.12).

Taking into account (3.12) we choose

$$\omega_0 = -B, \qquad \lambda_0 = 0. \quad (3.32)$$

As well-known,

$$\int_{|z|=1}\frac{1+z}{1-z}\frac{dz}{z} = \int_{|z|=1}\frac{1-z}{1+z}\frac{dz}{z} = 0. \quad (3.33)$$

Therefore, from (3.20), (3.27), (3.28), and (3.33) we have (see also (3.31) and (3.32))

$$\int_{-B}^{-B+\pi^2D^2/H^2} \frac{h_0(\omega)}{h_1(\omega)}\,d\omega = 0, \quad (3.34)$$

$$\int_{-B}^{-B+\pi^2D^2/H^2} \frac{h_1(\omega)}{h_0(\omega)}\frac{d\omega}{B+\omega} = 0. \quad (3.35)$$

Similarly, it is easy to verify that (see (3.27), (3.28), and (3.26))

$$\int_{-B}^{-B+\pi^2D^2/H^2} \frac{g_0(\omega)h_1(\omega) - g_1(\omega)h_0(\omega)}{(B+\omega)g_0(\omega)h_0(\omega) + D^2 g_1(\omega)h_1(\omega)}\,d\omega = 0, \quad (3.36)$$

$$\int_{-B}^{-B+\pi^2D^2/H^2} \frac{(B+\omega)g_0(\omega)h_0(\omega) + D^2 g_1(\omega)h_1(\omega)}{(B+\omega)(g_0(\omega)h_1(\omega) - g_1(\omega)h_0(\omega))}\,d\omega = 0 \quad (3.37)$$

in the case of the boundary conditions (3.21), (3.22).

Formulae (2.34), (2.35) (as well as (2.36), (2.37)) for the general boundary conditions) could be used to reconstruct the coefficients D and B.

Consider the following function

$$F_D(\omega) = \int_{\omega_0}^{\omega} h_0(\xi) h_1^{-1}(\xi)\, d\xi. \tag{3.38}$$

Relation (3.34) means that for $\omega_0 = -B$ the zero $\omega = A$ of this function ($F_D(A) = 0$) corresponds to the parameter D:

$$A = \omega_0 + \frac{\pi^2 D^2}{H^2}, \qquad D = \frac{H}{\pi}\sqrt{A - \omega_0}. \tag{3.39}$$

Having known D^2 we use an indirect function (3.35) to find the parameter B. In other words, original inverse problem for differential equation has been reduced to the system of two indirect equations (3.34), (3.35) or (3.36), (3.37). Such system does not deal with derivatives, only integrals are involved. The relations above have been derived only for the constant coefficients D and B. However, we will use this approach for preliminary evaluation of the problem parameters.

4. An algorithm for numerical inversion

As a first step to solve the Inverse Problem (2.2)–(2.5) numerically, we apply the Laplace transform. As it has been shown in the previous section, replacing the original dynamical problem with the Helmholtz equation is correct at least in some cases. The point is that recovering the space-dependent coefficients, $D(z)$ and $B(z)$, in the frequency domain, we do not need to go back to time domain. Therefore, we shall not deal with the delicate task of the inverting Laplace transforms which is far nontrivial in itself. Here we used the term frequency domain retaining a formal analogy with inverse problems for the wave equation, in which case the frequency domain concerning Fourier images of solutions has a clear physical meaning (see [1], [3]).

For simplicity, below we assume $z \geq 0$ and $\omega \in [\omega_1, \omega_2]$. The coefficients $D(z)$ and $B(z)$ are supposed to be smooth, $D(z), B(z) \in C^2(0, \infty)$, say, and the constant for the sufficiently large values of z, $D(z) = D_\infty = \text{const}$, $B(z) = B_\infty = \text{const.}$ for $z \geq H$.

Consider the following problem:

$$\frac{d^2 v}{dz^2} + \frac{B(z) + \omega}{D^2(z)} v = 0, \tag{4.1}$$

$$\left.\frac{dv}{dz}\right|_{z=0} = F(\omega), \quad v|_{z=H} = 0, \tag{4.2}$$

where $v(z,\omega) = \int\limits_0^\infty e^{\omega t}\delta X\, dt$ and $F(\omega) = \int\limits_0^\infty e^{\omega t}\varphi_1(t)\, dt$ (cf. (2.2)–(2.5)).

The inverse problem, we are interested in, consists in reconstruction of both functions $D(z)$ and $B(z)$ by using the additional piece of information

$$v_0(\omega) = v(0,\omega), \quad \omega_1 \le \omega \le \omega_2, \tag{4.3}$$

where $[\omega_1,\omega_2]$ is the interval of available frequencies.

We solve the inverse problem (4.1)–(4.3) by minimizing the cost functional

$$\Phi[D,B] = \int\limits_{\omega_1}^{\omega_2} \left|v_0(\omega) - K[D,B](\omega)\right|^2 d\omega + \beta \sup_z |D - D^{\mathrm{est}}| + \gamma \sup_z |B - B^{\mathrm{est}}|, \tag{4.4}$$

where the operator $K[D,B](\omega)$ maps the current "test" values of $D(z)$ and $B(z)$ into the solution to the boundary value problem (4.1), (4.2), evaluated at the point $z = 0$. Here β and γ are some weighting regularization parameters, $0 \le \beta \le 1$, $0 \le \gamma \le 1$, and D^{est} and B^{est} are estimated values of D and B, respectively, that could be obtained from physical measurements.

After rather technical calculations (omitted here, since, e.g., a similar approach can be found in [11]), we obtain the following formulae for the gradients of the cost functional with respect to D and B:

$$(\nabla_D \Phi[D,B])(z) = -2\,\mathrm{Re} \int\limits_{\omega 1}^{\omega 2} (B(z)+\omega)\overline{F}(\omega) \times [v_0(\omega) - F(\omega)G(0,\omega)]\overline{G}^2(z,\omega)\, d\omega, \tag{4.5}$$

$$(\nabla_B \Phi[D,B])(z) = -2\,\mathrm{Re} \int\limits_{\omega 1}^{\omega 2} D^{-2}(z)\overline{F}(\omega) \times [v_0(\omega) - F(\omega)G(0,\omega)]\overline{G}^2(z,\omega)\, d\omega. \tag{4.6}$$

Here $G(z,\omega)$ solves the problem

$$\frac{d^2G}{dz^2} - \frac{B(z)+\omega}{D^2(z)} G = 0, \qquad \left.\frac{dG}{dz}\right|_{z=0} = 1, \quad G|_{z=H} = 0.$$

By a bar over F and G we mean taking the complex conjugate.

Here, we do not consider the complicated theoretical question of uniqueness as well as of existence of the *global* minimum point of the cost functional (4.4). We refer, instead, the reader to the paper [12], in which similar questions have been discussed.

The following modification of the conjugate gradient method has been used to minimize the cost functional (4.4):

$$D_{k+1}(z) = D_k(z) - \alpha_k P_k(z), \tag{4.7}$$

$$\alpha_k = \arg\min_{\alpha>0} \Phi[D_k - \alpha P_k, B], \tag{4.8}$$

$$P_0(z) = \nabla_D \Phi[D_0, B], \tag{4.9}$$

$$P_k(z) = \nabla_D \Phi[D_k, B](z) - \tau_k P_{k-1}(z), \quad k \geq 1, \tag{4.10}$$

$$\tau_k = (\nabla_D \Phi[D_k, B], \nabla_D \Phi[D_{k-1}, B] - \nabla_D \Phi[D_k, B]); \tag{4.11}$$

$$B_{k+1}(z) = B_k(z) - \alpha_k P_k(z), \tag{4.12}$$

$$\alpha_k = \arg\min_{\alpha>0} \Phi[D, B_k - \alpha P_k], \tag{4.13}$$

$$P_0(z) = \nabla_D \Phi[D, B_0], \tag{4.14}$$

$$P_k(z) = \nabla_D \Phi[D, B_k](z) - \tau_k P_{k-1}(z), \quad k \geq 1, \tag{4.15}$$

$$\tau_k = (\nabla_D \Phi[D, B_k], \nabla_D \Phi[D, B_{k-1}] - \nabla_D \Phi[D, B_k]), \tag{4.16}$$

where k is the iteration number and the step α_k is chosen by the"golden section" method.

5. Numerical experiments

Computer codes have been prepared in C++, while Mathematica 3.0 has been used for verification and visualization. All this can be run on personal computers. Four different numerical experiments have been performed. On each iteration, the function $\delta X(z, \omega)$ has been computed by the so-called semi-analytical method described in [12].

In the first experiment, we consider two rather complicated models for $D(z)$, with $B(z) \equiv 1$ (i.e., with a constant value for B). The space interval $0 \leq z \leq H$ ($H = 650$ meters) has been divided into 13 layers with identical thickness of 50 meters.

The regularization parameter $\beta = 0.2$ provided the best convergence rate of the iterative process; 38 iterations of the conjugate gradient method (3.7)–(3.11) were made in order to reconstruct the function $D(z)$ for the first model (Figure 1), and 41 iterations were needed for the second model (Figure 2).

In the second series of tests, the simpler model for $D(z)$ has been considered, but the coefficient $B(z)$ has been chosen as shown in Figure 4. Here the values of $B(z)$ were assumed to be known. Now, 5 layers were considered, each one of 200 meters. In Figure 3, the result of reconstruction of $D(z)$ after 34 iterations is shown. The regularization parameter β was taken equal to 0.5.

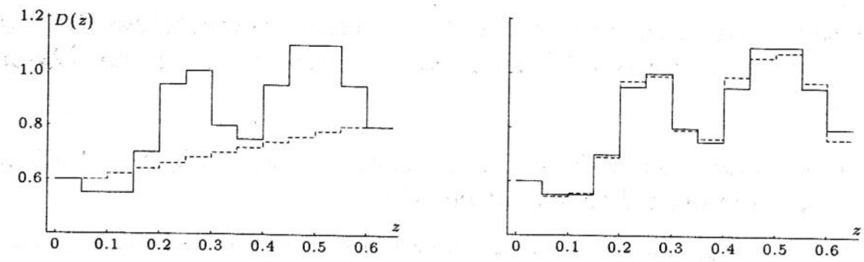

Figure 1. Reconstruction of the coefficient $D(z)$ in a simplified model with $B \equiv 1$. The solid line shows $D(z)$, while the dashed line represents the initial approximation (left part), and the result of numerical inversion (right part)

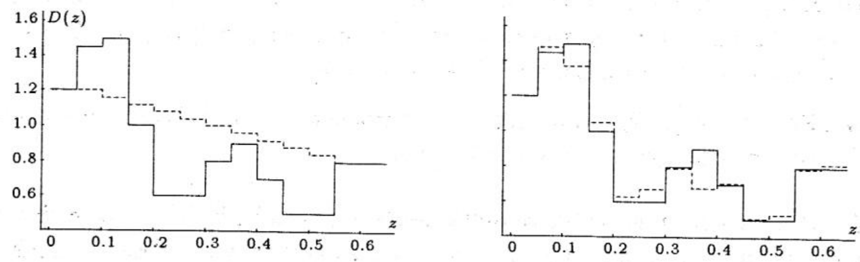

Figure 2. Numerical results, as in Figure 1, with an alternative choice for $D(z)$

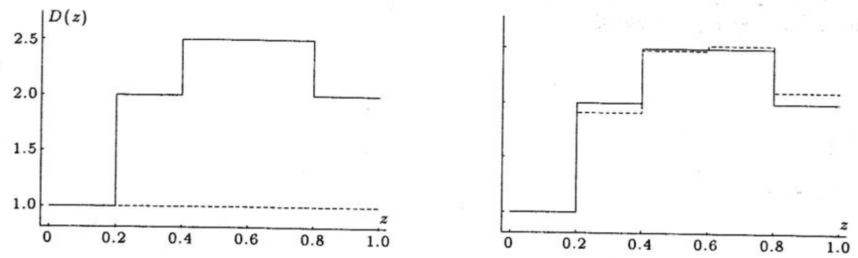

Figure 3. Numerical test for a case of $B(z) \neq 1$. Only the coefficient $D(z)$ has been reconstructed. For the values of $B(z)$, see the next figure

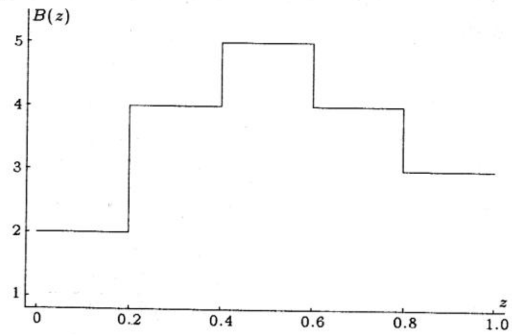

Figure 4. Values of the coefficient $B(z)$, cf. Figure 3

In the third series of experiments, the unknown coefficients $D(z)$ and $B(z)$ have been reconstructed simultaneously. Here we used the following scheme:

Step 1 Estimate the initial values of $D(z)$ and $B(z)$ from (3.36), (3.37), and fix the values of the coefficient $B(z)$.

Step 2 Try to reconstruct $D(z)$ by the method of conjugate gradient, (3.7)–(3.11), stopping the iterative process when the values of the cost functional does not change appreciably (within a prescribed accuracy).

Step 3 Keep fixed the so-obtained value of $D(z)$, and try to recover the coefficient $B(z)$ by the method of conjugate gradient, (3.12)–(3.16), stopping the iteration proceeding as above.

Step 4 Repeat Steps 2 and 3 until the so-obtained functions $D(z)$ and $B(z)$ do not change appreciably (as above).

We tried to reconstruct the coefficients $D(z)$ and $B(Z)$, approximating them by piecewise constant functions, over 6 layers, whose width is about 200 meters. The regularization parameters, β and γ, were chosen equal to 0.3 and 0.2, respectively. The final results, achieved after 98 iterations, are shown in Figures 5 and 6.

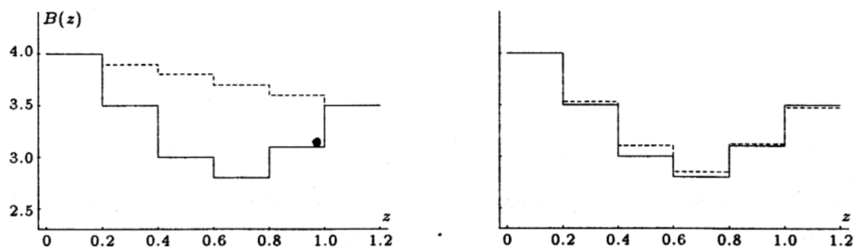

Figure 5. Simultaneous reconstruction of both coefficients, $D(z)$ and $B(z)$. Here the coefficient $B(z)$ is shown

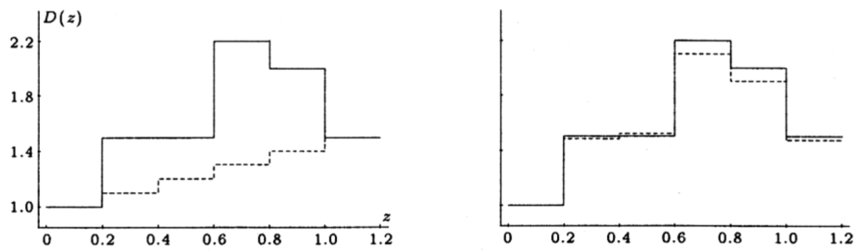

Figure 6. Results of the numerical reconstruction of the diffusion coefficient $D(z)$, cf. Figure 5

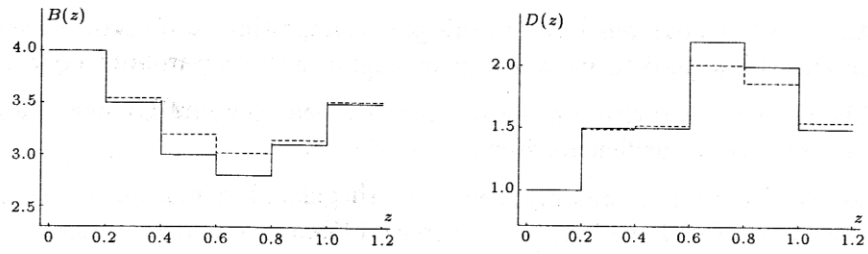

Figure 7. Results of simultaneous reconstruction of the coefficients $D(z)$ and $B(z)$. The initial approximations have been chosen as in Figure 5, 6. Moreover, a normally distributed random noise in the range of 5%, has been added to the inversion data

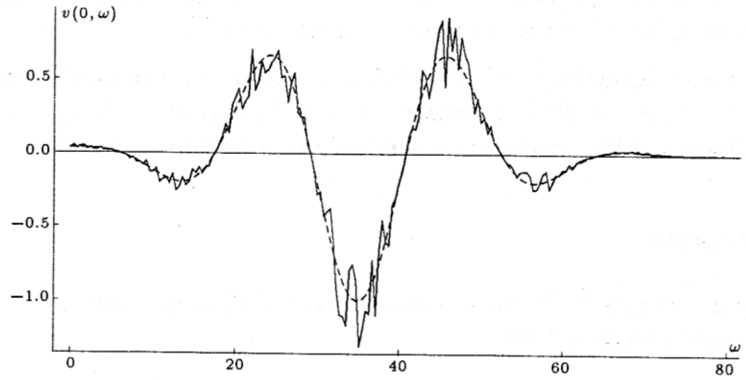

Figure 8. The inversion data (trace of solution of the direct problem at the point $z = 0$) is represented as a dashed line. The solid line shows corrupted inversion data, cf. Figure 7

In order to test the robustness of the algorithm, the inversion data have been artificially corrupted by adding some amount of noise. This has been done in the last series of numerical experiments, where the same model considered in the third test has been treated. Here, however, a normally distributed random noise whose average fluctuations were equal to 5% of the data amplitudes, has been superimposed to to the inversion data (Figure 8). The result of the simultaneous identification of *two* coefficients are shown in Figure 7. The initial approximations for $D(z)$ and $B(Z)$ were the same as in the previous test, see Figures 5 and 6.

6. Conclusions

In closing, the following points should be stressed:

1. At the present time, only a few results concerning the mathematical use of the Laplace transforms for the inverse problems have been obtained.

2. As it has been demonstrated in this paper, an optimization procedure can be effectively used to recover a given coefficient of a parabolic equation.
3. The inversion algorithm proposed here has been successfully used *also* to determine *two* coefficients simultaneously.
4. Issues of existence and uniqueness of the global minimum of the cost functional (4.4) have not been addressed. Both these questions are very complicated and a separate mathematical analysis is required.
5. Convergence of the iterative process has been investigated only numerically. The regularization parameters, β and γ, have also been chosen experimentally, without any rigorous mathematical background. These questions also call for a special theoretical analysis.
6. An *a priori* knowledge of the global variations of the coefficients $D(z)$ and $B(z)$ (the so-called "trend components") may essentially improve the convergence of the inversion procedure described in this paper.

References

[1] Aki K., Richards P. G. Quantitative Seismology, Theory and Methods. – San Francisco: Freeman, 1980.

[2] Lavrent'ev M. M., Romanov V. G., Shishatskii Ill-Posed Problems of Mathematical Physics and Analysis // AMS Translations of Math. Monographs. – 1986. – Vol. 64.

[3] Avdeev A. V., Lavrentiev M. M., Priimenko, V. I. Inverse Problems and Some Applications. – Novosibirsk: ICMMG, 1999.

[4] Capobianco M. A procedure for parameter identification of partial differential equations of parabolic type // G6-M Workshop "System Dynamics", Delft Hydraulics, April 27–29, 1992.

[5] De Vriend H.J., Capobianco M., Chesher T., de Swart H.E., Latteux B., Stive M.J.F. Approaches to long-term modelling of coastal morphology: a review // Coastal Engineering. – Amsterdam: Elsevier Science Publ. B.V., 1993. – № 21. – P. 225–269.

[6] Yakhno V. G. Inverse Problems for Differential Equations of Elasticity. – Novosibirsk: Nauka, 1992 (in Russian).

[7] Hanson H. GENESIS, a generalized shoreline change numerical model for engineering use. – 1987. – (Report / Univ. of Lund, Dept. of Water Res. Eng.; 1007).

[8] Dean R.G. Equilibrium beach profiles: characteristics and applications // J. Coastal Res. – 1991. – Vol. 7, № 1. – P. 53–84.

[9] Larson M., Hanson H., Kraus N.C. Analytical solutions of the one-line model of shoreline change: Report to U.S. Army Corps of Engineers. – Coastal Engineering Research Center, 1987.

[10] Bakker W.T. The dynamics of a coast with a groyne system // Proc. of the 11th Coastal Engineering Conference. – American Society of Civil Engineers, 1968. – P. 492–517.

[11] McGillivray P.R., Oldenbourgh D.W. Methods for calculating Freché derivatives and sensitivities for the nonlinear inverse problems: a comparative study geophysical prospecting. – 1990. – Vol. 38, № 5. – P. 499–524.

[12] Alekseev A.S., Avdeev A.V., Fatianov A.G., Cheverda V.A. Wave processes in vertically inhomogeneous media: a new strategy for a velocity inversion // Inverse Problems. – 1993. – Vol. 9, № 3.

[13] Romanov V.G. Inverse Problems of Mathematical Physics. – Moscow: Nauka, 1989 (in Russian).